Decorating multi-walled carbon nanotubes with quantum dots for construction of multi-color fluorescent nanoprobes

2010 Nanotechnology 21 045606

(http://iopscience.iop.org/0957-4484/21/4/045606)

Nanotechnology **21** (2010) 045606 (8pp) doi:10.1088/0957-4484/21/4/045606

Decorating multi-walled carbon nanotubes with quantum dots for construction of multi-color fluorescent nanoprobes

Nengqin Jia[1,3], Qiong Lian[1], Zhong Tian[1], Xin Duan[2], Min Yin[1], Lihong Jing[2], Shouhui Chen[1], Hebai Shen[1] and Mingyuan Gao[2,3]

[1] Department of Chemistry, Life and Environmental Science College, Shanghai Normal University, Shanghai 200234, People's Republic of China
[2] Institute of Chemistry, Chinese Academy of Sciences, Beijing 100190, People's Republic of China

E-mail: nqjia@shnu.edu.cn and gaomy@iccas.ac.cn

Received 29 August 2009, in final form 22 November 2009
Published 16 December 2009
Online at stacks.iop.org/Nano/21/045606

Abstract

Novel multi-color fluorescent nanoprobes were prepared by electrostatically assembling differently sized CdTe quantum dots on polyethylenimine (PEI) functionalized multi-walled carbon nanotubes (MWNTs). The structural and optical properties of the nano-assemblies (MWNTs–PEI–CdTe) were characterized by transmission electron microscopy (TEM), electron diffraction spectra (EDS), Raman spectroscopy, confocal microscopy and photoluminescence spectroscopy (PL), respectively. Electrochemical impedance spectroscopy (EIS) was also applied to investigate the electrostatic assembling among oxidized MWNTs, PEI and CdTe. Furthermore, confocal fluorescence microscopy was used to monitor the nano-assemblies' delivery into tumor cells. It was found that the nano-assemblies exhibit efficient intracellular transporting and strong intracellular tracking. These properties would make this luminescent nano-assembly an excellent building block for the construction of intracellular nanoprobes, which could hold great promise for biomedical applications.

(Some figures in this article are in colour only in the electronic version)

1. Introduction

Nanomaterials have shown great potentials in biomedical applications including detection, diagnosis and therapeutic systems. Towards these applications, semiconductor quantum dots (QDs) and carbon nanotubes (CNTs) have received intensive investigations. QDs have been demonstrated to be a new type of fluorescent labeling material superior to conventional dyes in many respects. For example, the fluorescence of QDs is generally characterized by narrow, symmetrical and particle-size-dependent features, as well as very broad excitation wavelength range, which make them very useful in high throughput biodetection and multi-color imaging [1–7]. Very recently, CNTs have also been demonstrated to be useful in a number of biological and biomedical applications due to their unique structures [8–19]. Therefore, by combining the attractive tubular structure with the fluorescent property, the QD-decorated carbon nanotube can be an ideal candidate for a multifunctional nanomaterial [20–27].

Herein, with the goal of exploring a potentially excellent scaffold for constructing intracellular multivalent nanoprobes for biomedical applications, we present a novel multi-color fluorescent nanoprobe prepared by electrostatic assembling differently sized CdTe on MWNTs (scheme 1). Due to the extremely high aspect ratio and the proton-sponge effects, the positively charged PEI–MWNTs could facilitate the loading and intracellular transporting of multi-color QDs containing both red and green CdTe nanocrystals. Simultaneous detection of two different-colored QD coatings on the nanotubes inside living cells was achieved by excitation by a single laser light source of 488 nm with appropriately chosen color channels by confocal fluorescence microscopy, avoiding the problems of

[3] Authors to whom any correspondence should be addressed.

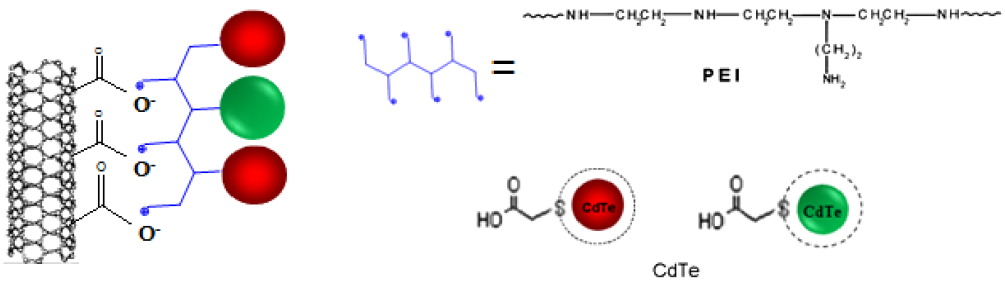

Scheme 1. The self-assembled structure of the MWNT–PEI–CdTe nanoprobe.

par-focality and image registration that are often encountered in multi-color fluorescence imaging [28, 29], which will benefit both imaging and tracking multiple targets simultaneously in living cells. Systematic results reveal that the multi-color nanoprobe exhibited highly aqueous dispersibility, intensive visible light emissions, efficient intracellular transport and strong intracellular tracking. Thus, the assembly of QDs with different emission colors onto MWNTs is an attractive strategy for enhancing their potential as biological fluorescent nanoprobes in cellular imaging. Moreover, it could be anticipated that the multi-color quantum dots decorated on one single MWNT would provide different binding sites to conjugate with various biological molecules and drugs (DNA, antibodies, siRNA, etc). Therefore, the MWNT–PEI–CdTe multi-color nanoprobes described in this study could also be extended to more sophisticated bioapplications such as multi-color coding, multiplexed assays and multi-targeted biomedical treatment by using carbon nanotubes as an internalization vehicle for carrying not only fluorescent probes but also functional biomaterials.

2. Experimental details

2.1. Materials

All reagents used were available commercially and were of high purity grade. MWNTs (95% purity, diameter 10–20 nm, length 1–2 μm) were purchased from Shenzhen Nanotech Port Co., Ltd. Polyethylenimine (PEI) (25 K) was obtained from Sigma-Aldrich. Water-soluble CdTe quantum dots with different colors were prepared by modifying the diameter of the particles based on our previously developed method [30–32].

2.2. Functionalization of MWNTs and characterization

MWNTs were suspended in a concentrated sulfuric acid/nitric acid mixture (3:1 v/v) and sonicated in a sonic bath for 16 h. After this treatment, the oxidized MWNTs were obtained after filtration and were then thoroughly rinsed. Then polyethylenimine (PEI) was used to modify the oxidized MWNTs to obtain functionalized MWNTs (PEI–MWNTs). 20 mg of oxidized MWNTs was mixed with 0.1% PEI solutions and sonicated for 15 min. After filtration and thorough washing with deionized water, the nanotubes were dispersed in water again at a concentration of 0.1 mg ml^{-1}.

Transmission electron microscopy (TEM) was carried out on a JEOL JEM 2100 with an acceleration voltage of 200 kV. Raman spectra of the aqueous suspensions were recorded using a Jobin Yvon MicroRaman with an excitation length of 632.8 nm.

2.3. Synthesis and characterization of MWNTs–PEI–CdTe

The MWNTs–PEI–CdTe nano-assemblies were synthesized as follows. 0.1 mg ml^{-1} PEI–MWNT solution was mixed with 1.3 mM mercaptoacetic acid-capped CdTe (610 nm red CdTe and 525 nm green CdTe) aqueous solution by reacting for 3 h with end-over-end rotation at room temperature. After filtration and thorough washing with deionized water, the MWNTs–PEI–CdTe were dispersed in water again. The negatively charged CdTe nanocrystals were then anchored to the surface of the positively charged PEI–MWNTs through the electrostatic interaction.

Morphology and composition of the MWNTs–PEI–CdTe were characterized using HRTEM and electron diffraction spectra (EDS). Photoluminescence (PL) measurements were carried out on a Varian Cary-Eclipse 500 spectrometer. To study the luminescence behavior of MWNTs–PEI–CdTe, a drop of MWNTs–PEI–CdTe suspension was smeared on a glass slide for fluorescent microscopy observed using confocal laser scanning microscopy (Carl Zeiss LSM 5 PASCAL). The emission was collected using 488 nm laser excitation and a 505–600 nm band-pass (BP) emission filter for green QDs and a 560 nm LP emission filter for red QDs.

2.4. Electrochemical assay of the electrostatically layer-by-layer assembling of MWNTs–PEI–CdTe

The glassy carbon electrode (GC, 3 mm in diameter) was polished to a mirror-like surface with 1.0, 0.3 and 0.05 μm alumina slurry followed by rinsing thoroughly with double distilled water. The electrodes were successively sonicated in 1:1 (v/v) nitric acid/water solution, acetone and double distilled water, and then allowed to dry at room temperature. A 20 μl of 0.1 mg ml^{-1} oxidized MWNT solution was dropped onto the surface of a pretreated GC electrode and dried under an infrared lamp to form the oxidized MWNT-modified electrode. For preparation of the PEI–MWNTs/GC modified electrode, the oxidized MWNT-modified electrode was dipped into 0.1% PEI solution for 3 h at room temperature, then the loosely bounded polymers were washed away with double distilled water. For preparation of CdTe–PEI–MWNTs/GC-modified electrode, the PEI–MWNTs/GC-modified electrode

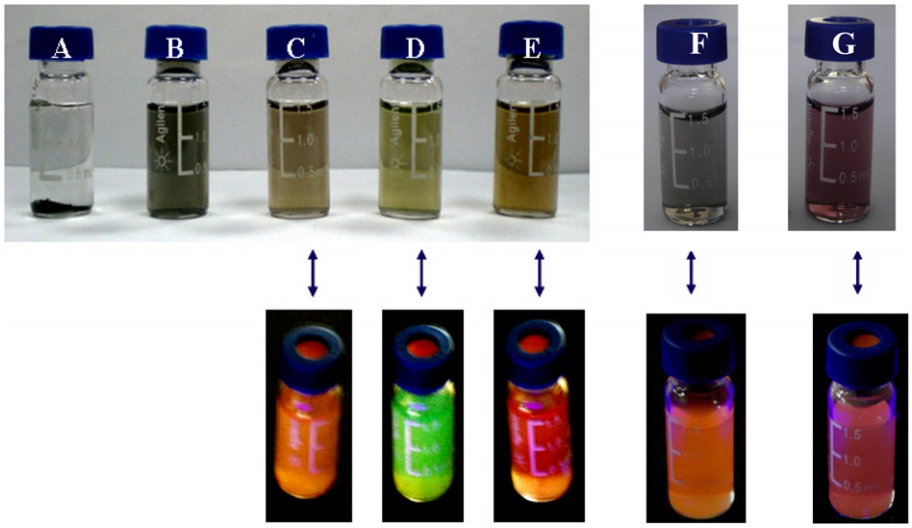

Figure 1. Upper panel: photographs of aqueous dispersions of (A) the pristine MWNTs in water, (B) MWNTs–PEI, (C) MWNTs–PEI–CdTe consisting of both green- and red-emission, (D) green-emission and (E) red-emission CdTe nanocrystals, respectively; MWNTs–PEI–CdTe consisting of both green- and red-emission CdTe nanocrystals in (F) PBS solution and (G) cell culture medium. Lower panel: photographs of the corresponding dispersions of the MWNTs–PEI–CdTe nanoprobes captured in UV light.

was dipped into 1.3 mM CdTe (610 nm red CdTe and 525 nm green CdTe) solution for 3 h, then the loosely bounded particles were washed away with double distilled water.

The electrochemical impedance spectroscopy (EIS) measurements were carried out by using an EG&G 5210 frequency response analyzer interfaced to a PAR Model 283 potentiostat (EG&G, TN, USA). The impedance measurements were performed in the presence of 10 mM $K_3Fe(CN)_6/K_4Fe(CN)_6$ by applying an ac voltage with 5 mV amplitude in a frequency range from 1 Hz to 100 kHz under open-circuit potential condition. The difference in electron transfer among the oxidized MWNTs/GC-modified electrode, PEI–MWNTs/GC-modified electrode and CdTe–PEI–MWNTs/GC-modified electrode was taken as the signal produced by the layer-by-layer electrostatic interaction among oxidized MWNTs, PEI and CdTe.

2.5. Cell internalization studies

Pulmonary carcinosis SPCA-1 cells were cultured in RPMI (Roswell Park Memorial Institute) 1640 medium supplemented with 10% fetal bovine serum (FBS). For confocal microscopy, the SPCA-1 cells were incubated with MWNTs–PEI–CdTe (1.25 mg l^{-1} MWNTs–PEI, 20 μM CdTe) solution for 1 h at 37 °C with 5% CO_2 on chambered slides. After that the cells were thoroughly washed, resuspended in RPMI 1640 medium and fetal bovine serum (FBS, 10%) and incubated for 3 h at 37 °C with 5% CO_2 atmosphere. After incubation, the cells were observed by confocal microscopy.

3. Results and discussion

Due to their hydrophobic nature, the surface modification of the carbon nanotubes was necessarily the first step for constructing nanotube-based fluorescent intracellular nanoprobes. In detail, a strong acid treatment was combined with a supersonication treatment for generating anionic carboxyl groups along the sidewall and both ends of the shortened nanotubes. The following polyethylenimine (PEI) modification achieved by electrostatic attraction can enhance the aqueous dispersibility of the resultant nanotubes, especially under physiological conditions, which is important for utilizing carbon nanotubes as the intracellular transporting carrier. Most importantly, the surface PEI modification also enabled the following self-assembly of differently sized CdTe nanocrystals on the surface of MWNTs–PEI, eventually leading to the nanoprobes shown in scheme 1.

Figure 1 presents photographs of aqueous dispersions of the pristine MWNTs, MWNTs–PEI and MWNTs–PEI–CdTe nanoprobes. It is quite evident that the pristine MWNTs possess very poor aqueous dispersibility. In contrast, the PEI modification enables the MWNTs as well as the MWNTs–PEI–CdTe to be well dispersible in aqueous solutions. The resultant colloidal solutions, shown in figure 1, presented excellent colloidal stability and remained practically unchanged for several months. Furthermore, the MWNTs–PEI–CdTe exhibited good stability in both PBS buffer solution and cell culture medium. Moreover, the fluorescent properties of the CdTe nanocrystals in the assembled structures were preserved. Under excitation of UV light (365 nm), the MWNTs–PEI–CdTe assembled structures consisting of different types of CdTe nanocrystals emit strong fluorescence of different colors. These results suggest that the current preparative processes are very effective in achieving well-dispersible MWNTs–PEI–CdTe assemblies.

The aggregation structure of the nanotubes was also investigated by TEM (figures 2(a), (b)). By comparing with pristine MWNTs, in the MWNTs–PEI sample, the entangling degree was tremendously reduced, with a large percentage of individual nanotubes being present. Moreover, the length

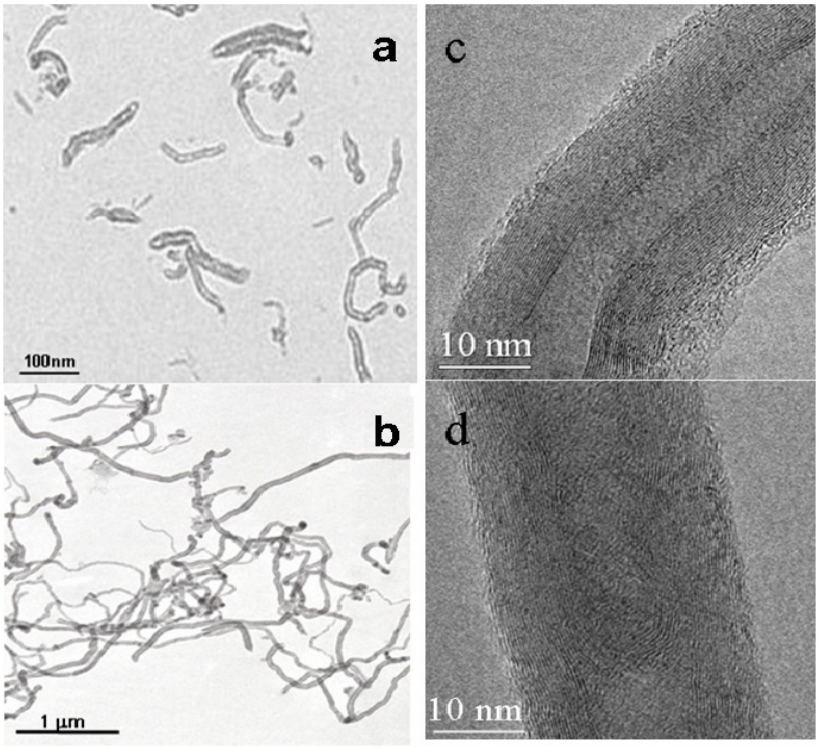

Figure 2. TEM and HRTEM images of aqueous dispersions of PEI–MWNTs ((a), (c)) and pristine MWNTs ((b), (d)).

of the MWNTs–PEI was greatly reduced to 50–150 nm, which is more suitable for intracellular delivery. Furthermore, comparing the HRTEM images shown in figures 2(c), (d), direct evidence for the presence of PEI on the MWNT surface can be found. The pristine MWNT surfaces are very smooth and demonstrate clear edges. In contrast, the MWNTs after PEI functionalization are fully covered by a uniform amorphous polymer layer, which results from the adsorption of PEI.

The PEI modification on MWNTs was further investigated by Raman spectroscopy which is a useful tool for probing the structural and electronic properties of carbon nanotubes [22]. The results are shown in figure 3. Both the MWNT and PEI–MWNT samples exhibit typical Raman characteristics of MWNTs with a tangential G band appearing in 1550–1605 cm^{-1} and a disorder-induced D band appearing at around 1350 cm^{-1}. It is known that the G band corresponds to the Raman-active E_{2g}, which is due to the vibration mode corresponding to the movement in opposite directions of two neighboring carbon atoms in a single-crystal graphite sheet, while the D band is associated with the presence of defects in the graphite layer [33]. It is evident that both G and D bands of PEI–MWNTs shift to higher wavenumbers, i.e. from 1566 to 1579 cm^{-1} for the G band and from 1319 to 1329 cm^{-1} for the D band, respectively. These shifts suggest that PEI is effectively coated on MWNTs. Since the strong attraction increases the energy necessary for vibrations to occur, it consequently leads to the up-shifts of the Raman peaks [34]. In addition, the relative intensity ratio of the D and G bands (I_D/I_G ratio) is widely used as a measure of sidewall covalent derivatization or defect introduction [35, 36]. The PEI modification also leads to a decrease of the I_D/I_G ratio from 1.22 to 1.01, suggesting that PEI is attached to the sidewall of the MWNTs via noncovalent bonds.

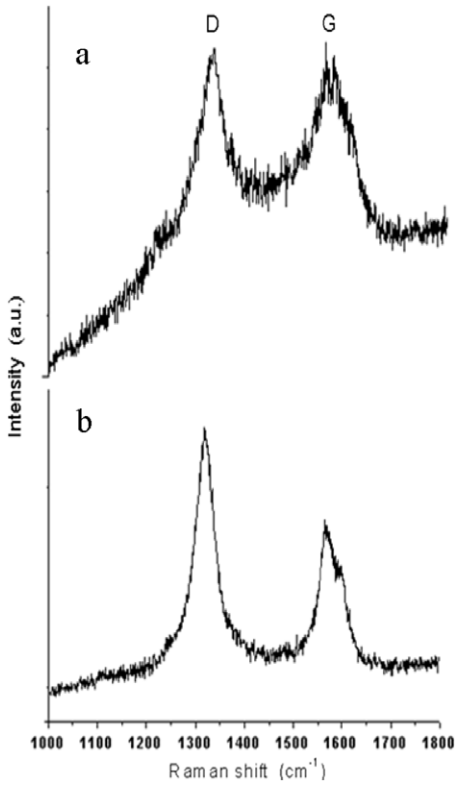

Figure 3. Raman spectra of the MWNTs after (a) and before being coated with PEI (b).

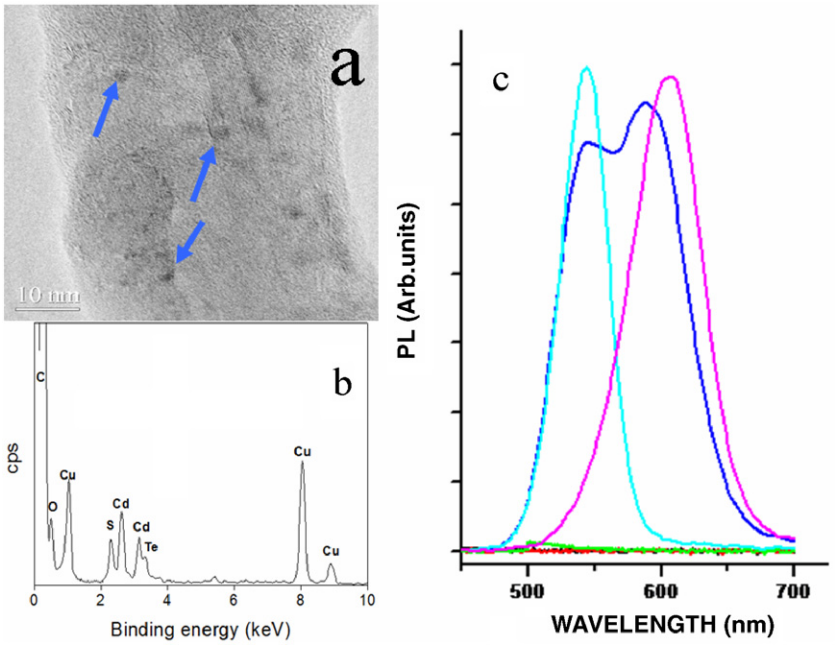

Figure 4. Left panel: HRTEM image (a) and EDS spectrum (b) of the MWNTs–PEI–CdTe. Blue arrows indicate the CdTe nanocrystals; right panel: (c) photoluminescence spectra of MWNTs (black line), MWNTs–PEI (red line), PEI (green line) and MWNTs–PEI–CdTe consisting of red CdTe (magenta line) and green CdTe (cyan line), respectively. The blue line is recorded from the MWNTs–PEI–CdTe sample consisting of both red and green CdTe nanocrystals. The excitation wavelength is 340 nm.

The assembled structure of MWNTs–PEI–CdTe was characterized by HRTEM and EDS. Figure 4(a) presents a TEM image of the MWNTs–PEI–CdTe sample containing two differently sized CdTe nanocrystals with fluorescence peak positions centering at 610 nm (red CdTe) and 525 nm (green CdTe), respectively. The molar ratio between them is 1:1. They appear as black dots in figure 4(a). The EDS measurements (figure 4(b)) reveal that the following elements, i.e. Cu, Cd, Te, S, O and C, are present in the inspected region. The Cu signal comes from the copper grid; O and part of the C signals can be attributed to the oxidized MWNTs; while Cd, Te and S signals come from CdTe nanocrystals which are stabilized by thioglycolic acid. Furthermore, the assembling process of the CdTe nanocrystals on the surface of PEI–MWNTs via electrostatic interactions can also be confirmed by electrochemical impedance spectroscopy (EIS) [37, 38] measurements shown in figure 5. It shows representative Nyquist diagrams of the electrochemical impedance spectra of the oxidized MWNTs/GC-modified electrode (curve a), PEI–MWNTs/GC-modified electrode (curve b) and CdTe–PEI–MWNTs/GC-modified electrode (curve c) in the presence of $[Fe(CN)_6]^{3-/4-}$ as a redox probe. As shown in figure 5, each of the three impedance spectra includes a semicircular portion and a linear line portion, which correspond to the electron-transfer process and diffusion process, respectively. The diameter of the semicircle represents the electron-transfer resistance at the electrode surface. The electron-transfer resistances of the oxidized MWNTs/GC-modified electrode, PEI–MWNTs/GC-modified electrode and CdTe–PEI–MWNTs/GC-modified electrode were 61, 40 and 118 Ω, respectively, exhibiting this layer-by-layer assembling process on the surfaces of the MWNTs. The EIS results suggest that the

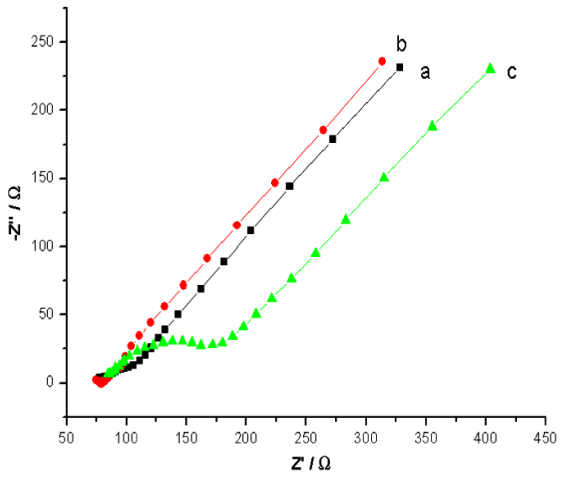

Figure 5. Nyquist plots for electrochemical impedance spectroscopy (EIS) measurements of a GC electrode in the presence of 10 mmol l^{-1} $[Fe(CN)6]^{3-/4-}$ with 0.1 mol L^{-1} KCl as the supporting electrolyte: (a) modified with oxidized MWNTs; (b) modified with MWNTs–PEI; (c) modified with MWNTs–PEI–CdTe.

PEI and the CdTe were successively adsorbed on the MWNTs by electrostatic interaction, which can be explained by the positively charged PEI polymer coating on the surface of the MWNTs facilitating the electron transfer of the $Fe(CN)_6^{3-/4-}$ redox couple and further adsorption of negatively charged CdTe relatively restricted the electron transfer of this redox couple.

The optical properties of the MWNTs–PEI–CdTe assemblies consisting of differently sized CdTe nanocrystals were

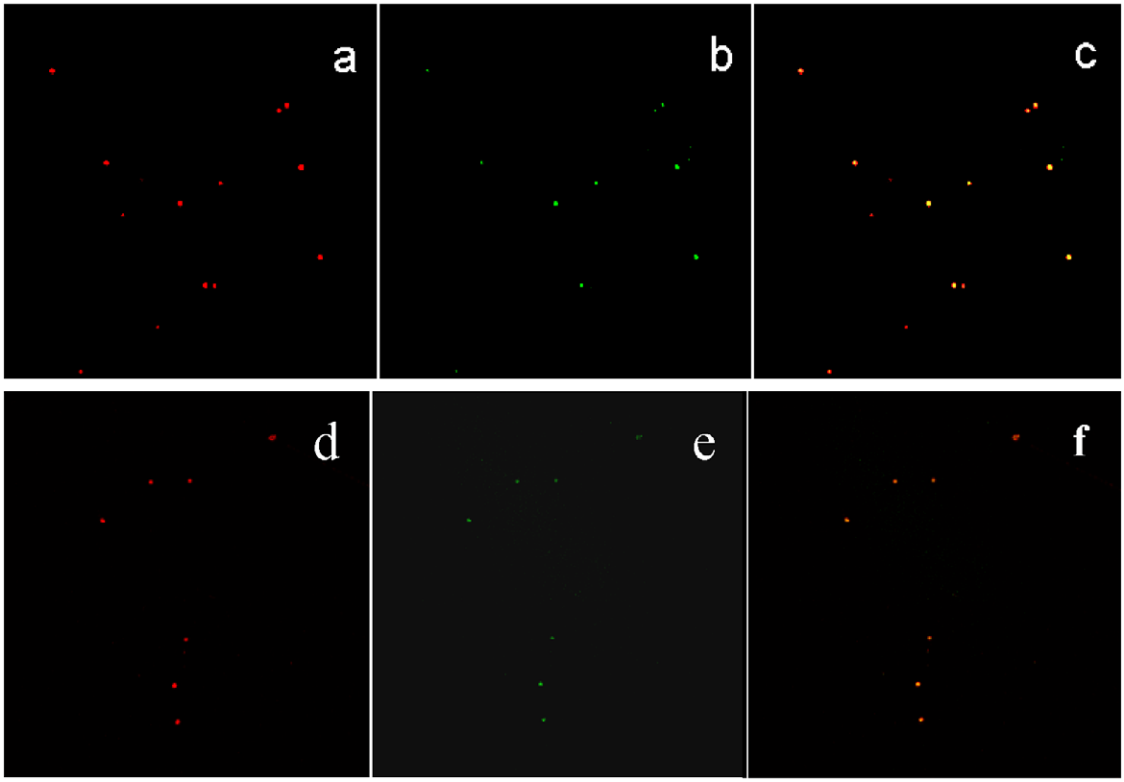

Figure 6. Confocal fluorescence images of MWNTs–PEI–CdTe nano-assemblies simultaneously assembled with red CdTe and green CdTe as prepared (upper panel), and dispersed in water for 3 days (lower panel). The emission was collected using 488 nm laser excitation. ((a), (d)) A 560 nm LP emission filter for red CdTe, ((b), (e)) a 505–565 nm band-pass (BP) emission filter for green CdTe, ((c), (f)) merged image.

characterized by fluorescence spectroscopy. As shown in figure 4(c), the PL spectrum of MWNTs–PEI–CdTe nano-assemblies displays the double-QD emission peaks similar to the characteristic luminescence peak for red/green CdTe nanocrystals, and a small PL peak shift of the nano-assemblies was possibly attributed to Förster resonance energy transfer (FRET) from small (green CdTe) to larger sized (red CdTe) nanocrystals [39] in the MWNTs–PEI–CdTe assemblies. The results suggest that the assembly of CdTe nanocrystals on the surface of the nanotube is, in principle, independent of the particle size.

Most importantly, the confocal fluorescence measurements on a single nanotube revealed that the stable fluorescence emissions of differently sized CdTe nanocrystals co-existed in the MWNTs–PEI–CdTe sample consisting of both red and green CdTe nanocrystals and the nano-assemblies keep good stability in conjugated form in water solution (figure 6). In addition, the nano-assemblies also exhibited relatively stable fluorescence characteristics in cell culture medium over a period of time observed by confocal fluorescence microscopy.

Following these investigations, we further assessed the ability of the multi-color nanoprobes to act as suitable labels for biological imaging and their potential for penetration of the cell membrane. Confocal microscopy was used to investigate the internalization of the nanoprobes into the pulmonary carcinosis SPCA-1 cells. As shown in figure 7, a large amount of orange dots were observed inside the living cells (merged image c). Red and green CdTe nanocrystals loading on the nanotubes inside the living cells were simultaneously detected upon excitation by a single laser light source of 488 nm with appropriately chosen color channels in confocal fluorescence microscopy (images a, b), suggesting the PEI–MWNTs loading the red QDs and green QDs can effectively transport into living cells. The possible insertion mechanism of the multi-color nanoprobes into the cells is considered to be through an endocytosis process as previously reported [19, 40]. Therefore, the current nanoprobes can be used as efficient luminescent nanoprobes for intracellular fluorescence labeling and would be an ideal candidate for a multifunctional nanomaterial for biomedicine applications.

4. Conclusions

In summary, a facile approach has been developed for constructing a new type of multi-color fluorescent nanoprobe consisting of MWNTs and fluorescent CdTe nanocrystals by electrostatically layer-by-layer assembling. In the self-assembled fluorescent nanoprobe, MWNTs serve as an intracellular vehicle, while CdTe nanocrystals serve as fluorescent probes. The multi-color fluorescent nanoprobes exhibit good aqueous dispersibility and stability, efficient intracellular transporting and strong intracellular tracking. Therefore, this novel MWNTs–PEI–CdTe complex represents a potentially excellent scaffold for constructing intracellular

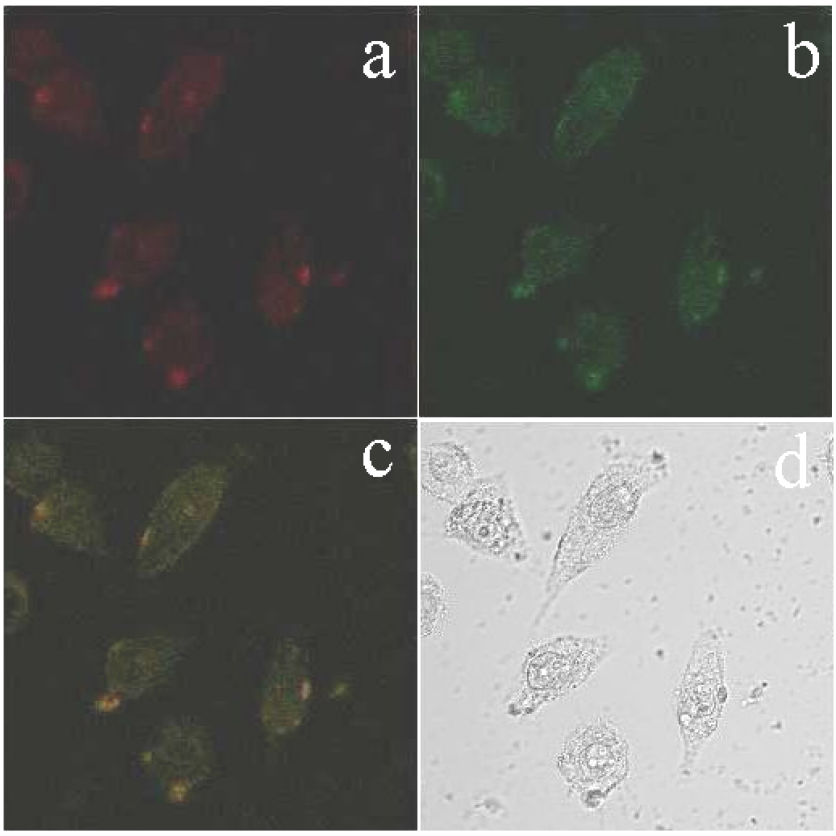

Figure 7. Confocal microscopy images of pulmonary carcinosis cells labeled by MWNTs–PEI–CdTe probe consisting of both red and green CdTe nanocrystals. Images (a) and (b) were captured by optically filtering the fluorescence of the second nanocrystals, while the merged image (c) shows the fluorescence from both green and red CdTe nanocrystals attached on the nanotubes. Image (d) is the phase image of the corresponding cells. The incubation time was 3 h. Details are provided in the experimental section.

multivalent nanoprobes, which could be of great promise for biomedical diagnosis and treatment.

Acknowledgments

This work was supported financially by LADP-SHNU (DZL806), NSFC (20773088 and 20773140), the National Basic Research Program of China (2008CB617504), the Program for New Century Excellent Talents in University (NCET-08-0897) and the Shanghai Sci. & Tech. and Education Committee (08QH14020, 09zz137 and S30406).

References

[1] Bruchez M Jr, Moronne M, Gin P, Weiss S and Alivisatos A P 1998 *Science* **281** 2013
[2] Michalet X, Pinaud F F, Bentolila L A, Tsay J M, Doose S, Li J J, Sundaresan G, Wu A M, Gambhir S S and Weiss S 2005 *Science* **307** 538
[3] Medintz I L, Uyeda H T, Goldman E and Mattoussi H 2005 *Nat. Mater.* **4** 437
[4] Derfus A M, Chan W C W and Bhatia S N 2004 *Adv. Mater.* **16** 961
[5] Murray C B, Kagan C R and Bawendi M G 2000 *Annu. Rev. Mater. Sci.* **30** 545
[6] Nirmal M and Brus L E 1999 *Acc. Chem. Res.* **32** 407
[7] Chan W C W and Nie S M 1998 *Science* **281** 2016
[8] Bianco A and Prato M 2003 *Adv. Mater.* **15** 1765
[9] Park K H, Chhowalla M, Iqbal Z and Sesti F 2003 *J. Biol.Chem.* **278** 50212
[10] Williams K A, Veenhuizen P T M, de la Torre B G, Eritjia R and Dekker C 2002 *Nature* **420** 761
[11] Pantarotto D, Briand J-P, Prato M and Bianco A 2004 *Chem. Commun.* **1** 16
[12] Zheng M *et al* 2003 *Science* **302** 1545
[13] Richard C, Balavoine F, Schultz P, Ebbesen T W and Mioskowski C 2003 *Science* **300** 775
[14] Martin C R and Kohli P 2003 *Nat. Rev. Drug Discovery* **2** 29
[15] Kam N W S, Liu Z and Dai H J 2005 *J. Am. Chem. Soc.* **127** 12492
[16] Liu Z, Winters M, Holodniy M and Dai H J 2007 *Angew. Chem. Int. Edn* **46** 2023
[17] Pantarotto D, Singh R, Mccarthy D, Erhardt M, Briand J-P, Prato M, Kostarelos K and Bianco A 2004 *Angew. Chem. Int. Edn* **43** 5242
[18] Yang D-Q, Rochette J-F and Sacher E 2005 *J. Phys. Chem.* B **109** 4481
[19] Jia N Q, Lian Q, Shen H B, Wang C, Li X Y and Yang Z N 2007 *Nano Lett.* **7** 2976
[20] Ravindran S, Chaudhary S, Colburn B, Ozkan M and Ozkan C S 2003 *Nano Lett.* **3** 447
[21] Li Q, Sun B, Kinloch I A, Zhi D, Sirringhaus H and Windle A H 2006 *Chem. Mater.* **18** 164
[22] Liu Y, Gao L and Sun J 2007 *J. Phys. Chem.* C **111** 1223
[23] Shi D, Guo Y, Dong Z Y, Lian J, Wang W, Liu G, Wang L and Ewing R C 2007 *Adv. Mater.* **19** 4033
[24] Olek M, Busgen T, Hilgendorff M and Giersig M 2006 *J. Phys. Chem.* B **110** 12901

[25] Bottini M, Cerignoli F, Dawson I M, Magrini A, Rosato N and Mustelin T 2006 *Biomacromolecules* **7** 2259
[26] Haremza M J, Hahn A M and Krauss D T 2002 *Nano Lett.* **2** 1253
[27] Banerjee S and Wong S S 2003 *J. Am. Chem. Soc.* **125** 10342
[28] Lacoste T D, Michalet X, Pinaud F, Chemla D S, Alivisatos A P and Weiss S 2000 *Proc. Natl Acad. Sci. USA* **97** 9461
[29] Agrawal A, Deo R, Wang G D, Wang M and Nie S 2008 *Proc. Nat. Acad. Sci. USA* **105** 3298
[30] Gao M Y, Kirstein S, Mohwald H, Rogach A L, Kornowski A, Eychmuller A and Weller H 1998 *J Phys. Chem.* B **102** 8360
[31] Yang Y H and Gao M Y 2005 *Adv. Mater.* **17** 2354
[32] Bao H B, Gong Y J and Gao M Y 2004 *Chem. Mater.* **16** 3853
[33] Georgakilas V, Voulgaris D, Vazquez E, Prato M, Guldi D M, Kukovecz A and Kuzmany H 2002 *J. Am. Chem. Soc.* **124** 14318
[34] Sinani V A, Gheith M K, Yaroslavov A A, Rakhnyanskaya A A, Sun K, Mamedov A A, Wicksted J P and Kotov N A 2005 *J. Am. Chem. Soc.* **127** 3463
[35] Dresselhaus M S, Dresselhaus G, Jorio A, Souza Filho A G and Saito R 2002 *Carbon* **40** 2043
[36] Ferrari A C and Robertson J 2000 *Phys. Rev.* B **61** 14095
[37] Ruan C, Yang L and Li Y 2002 *Anal. Chem.* **74** 4814
[38] Yang L, Li Y and Erf G F 2004 *Anal. Chem.* **76** 1107
[39] Clapp A R, Medintz I L and Mattoussi H 2006 *ChemPhysChem* **7** 47
[40] Kam N W, Liu S Z and Dai H 2006 *Angew. Chem. Int. Edn* **45** 577